Title

Estimating changes in urban ozone concentrations due to life cycle emissions from hydrogen transportation systems

Authors

Wang, Guihua
Ogden, Joan M
Chang, Daniel P.Y.

Publication Date

2007-12-01

Peer reviewed

Available online at www.sciencedirect.com
ScienceDirect
Atmospheric Environment 41 (2007) 8874–8890
ATMOSPHERIC ENVIRONMENT
www.elsevier.com/locate/atmosenv

Estimating changes in urban ozone concentrations due to life cycle emissions from hydrogen transportation systems

Guihua Wang[a,b,d,*], Joan M. Ogden[c,d], Daniel P.Y. Chang[a]

[a]*Department of Civil and Environmental Engineering, University of California, Davis, CA 95616, USA*
[b]*Department of Agricultural and Resource Economics, University of California, Davis, CA 95616, USA*
[c]*Department of Environmental Science and Policy, University of California, Davis, CA 95616, USA*
[d]*Institute of Transportation Studies, University of California, Davis, CA 95616, USA*

Received 3 April 2007; received in revised form 11 July 2007; accepted 10 August 2007

Abstract

Hydrogen has been proposed as a low polluting alternative transportation fuel that could help improve urban air quality. This paper examines the potential impact of introducing a hydrogen-based transportation system on urban ambient ozone concentrations. This paper considers two scenarios, where significant numbers of new hydrogen vehicles are added to a constant number of gasoline vehicles. In our scenarios hydrogen fuel cell vehicles (HFCVs) are introduced in Sacramento, California at market penetrations of 9% and 20%. From a life cycle analysis (LCA) perspective, considering all the emissions involved in producing, transporting, and using hydrogen, this research compares three hypothetical natural gas to hydrogen pathways: (1) on-site hydrogen production; (2) central hydrogen production with pipeline delivery; and (3) central hydrogen production with liquid hydrogen truck delivery. Using a regression model, this research shows that the daily maximum temperature correlates well with atmospheric ozone formation. However, increases in initial VOC and NO_x concentrations do not necessarily increase the peak ozone concentration, and may even cause it to decrease. It is found that ozone formation is generally limited by NO_x in the summer and is mostly limited by VOC in the fall in Sacramento. Of the three hydrogen pathways, the truck delivery pathway contributes the most to ozone precursor emissions. Ozone precursor emissions from the truck pathway at 9% market penetration can cause additional 3-h average VOC (or NO_x) concentrations up to approximately 0.05% (or 1%) of current pollution levels, and at 20% market penetration up to approximately 0.1% (or 2%) of current pollution levels. However, all of the hydrogen pathways would result in very small (either negative or positive) changes in ozone air quality. In some cases they will result in worse ozone air quality (mostly in July, August, and September), and in some cases they will result in better ozone air quality (mostly in October). The truck pathway tends to cause a much wider fluctuation in degradation or improvement of ozone air quality: percentage changes in peak ozone concentrations are approximately −0.01% to 0.04% for the assumed 9% market penetration, and approximately −0.03% to 0.1% for the 20% market penetration. Moreover, the 20% on-site pathway occasionally results in a decrease of about −0.1% of baseline ozone pollution. Compared to the current ambient pollution level, all three hydrogen pathways are unlikely to cause a serious ozone problem for market penetration levels of HFCVs in the 9–20% range.

Keywords: Life cycle analysis (LCA); Hydrogen; Natural gas (NG); Hydrogen pathways; Ozone formation; Ozone air quality

*Corresponding author. Department of Civil and Environmental Engineering, University of California, Davis, CA 95616, USA. Fax: +1 530 752 6572.
E-mail address: wghwang@ucdavis.edu (G. Wang).

1352-2310/$ - see front matter © 2007 Elsevier Ltd. All rights reserved.
doi:10.1016/j.atmosenv.2007.08.020

1. Introduction

Use of hydrogen as a transportation fuel has many potential benefits. Unlike gasoline, hydrogen can be derived from a variety of sources such as natural gas (NG), coal, biomass, electricity, solar, wind, and hydropower and could reduce oil supply insecurity; hydrogen fuel cell vehicles (HFCVs) do not have tailpipe emissions and as a result is environmentally friendly; if made from renewables, decarbonized fossil fuels, or nuclear energy, hydrogen can be produced and used with no emissions of greenhouse gases, and could help mitigate global warming; in addition, fuel cell vehicle running on hydrogen is up to 2.5 times as efficient as today's conventional internal combustion engine (ICE) vehicles (Ogden, 1999, 2002; Ogden et al., 2004; Sperling and Ogden, 2004).

Current mobile sources of pollution cause urban air quality degradation and damage to human health due to close proximity to people (Chaaban et al., 2001). Thus, it has been proposed that it would be promising and beneficial to introduce HFCVs into the vehicle marketplace in urbanized or populous regions. Assuming that, in a steady state, a certain number of HFCVs were operating in Sacramento County, California, this research investigates several possible fuel production pathways to satisfy the vehicular demand for hydrogen fuel. In light of resource availability and mainstream hydrogen production technology to date, steam-methane reforming (SMR) of NG is the only technology to produce hydrogen considered in the research.

HFCVs emit no tailpipe emissions, but there would be some emissions related to hydrogen considering the full fuel cycle, including hydrogen production and delivery. These processes directly emit primary criteria pollutants and precursors to secondary ozone, including NO_x (i.e., NO_2 and NO) and VOC (or called non-methane organic carbon, NMOC). Ozone is of concern because it is harmful to human health and agricultural crops and thus results in a social cost issue (ExternE, 1998; McCubbin and Delucchi, 1996; Delucchi et al., 1998; Delucchi and McCubbin, 2004).

In an earlier paper, the three common NG to hydrogen pathways were examined, and the incremental pollution of CO, SO_x, NO_x, PM_{10}, and VOC were estimated based on atmospheric physical transport of directly emitted pollutants, whereas no atmospheric chemical reactions like ozone formation were considered in that study (Wang et al., 2007). This research develops a region-specific regression model to predict atmospheric ozone formation. From a life cycle analysis (LCA) perspective, three hydrogen pathways are compared in terms of resulting changes in ozone pollution in urban Sacramento, and predictions of the potential ozone pollution caused by each of the hydrogen pathways relative to the current ambient pollution levels are produced.

2. Literature review on predictors of ozone formation

Ozone pollution and episodes mainly occur during the daylight hours of the summer months (NRC, 1991). In summary the "high ozone days" are likely affected by such parameters as ground level temperature, upper air temperature, dew point temperature, wind speed, wind direction, solar radiation or cloud cover, and relative humidity or precipitation (NRC, 1991). In addition to the meteorological conditions that lead to ozone episodes, the characteristics and chemical composition of VOC have an impact on ozone formation, and different species of VOC differ in their photochemical ozone creation potential (Derwent et al., 1996). Prediction of ozone formation has improved over the decades with the development of three-dimensional photochemical transport models, but they often include a hundred or more coupled reactions just to describe gas phase changes along with detailed meteorology, and yet may only yield results accurate to about 25%. For the purposes of this study a more efficient region-specific method of estimating the magnitude of the effects of different hydrogen pathways on ozone production was sought.

One such method might be to generate region-specific ozone isopleth data. Ideally, ozone isopleth diagrams can be produced by smog chamber experiments. In practice, the empirical kinetic modeling approach (EKMA) developed by the US EPA relates maximum hourly average ozone concentrations with the 6:00–9:00 am average of precursor concentrations in a region, and both standard and city-specific ozone isopleths can be generated (Kinoslan, 1982). From such studies it is recognized that the VOC and NO_x precursors to atmospheric ozone formation often yield a peak ozone when the VOC/NO_x ratio is around 7–10 (Chang et al., 1989), and that ozone formation is retarded by additional NO_x emissions when the

VOC/NO_x ratio is less than 5.5 (Seinfeld and Pandis, 1998).

Regression modeling approaches yield useful region-specific information when sufficient measurements are available. Based on daily air quality monitoring results for the downtown Los Angeles station for the months of August, September, and October, and using the 3-h (6–9 am) averages of total hydrocarbon and NO_x concentrations and the maximum hourly average oxidant concentration occurring on that day, an empirical model of ozone production was derived (Merz et al., 1972). Multiple regression modeling was also conducted to simulate the peak ozone produced by Los Angeles air in outdoor smog chambers, using the explanatory variables HC (i.e., hydrocarbon), NO_x, and the average daily temperature (Kelly and Gunst, 1990). That study was the first published to quantify the effect of temperature on peak ozone formation in captive air studies (Kelly and Gunst, 1990).

3. Methodology

3.1. Overview of methodology

This research develops a region-specific regression model to predict atmospheric ozone formation associated with a hydrogen transportation system. Our methodology has several steps.

First, we estimate the emissions of ozone precursors from the various steps (and locations) along selected hydrogen supply pathways. We then use an atmospheric dispersion model ISCST3 to find the precursor concentrations throughout the Sacramento area, using data for typical meteorological conditions. Next, we use the meteorological information and air quality data from 2004 to derive the relationship between ozone formation and its precursor concentrations by using regression analysis. Finally we use the regression-based model to estimate the incremental ozone concentrations due to hydrogen pathways.

This methodology should give a reasonable estimate of ozone concentrations in future years when hydrogen might be widely used, say in 2025 or beyond.[1]

[1]We used the 2004 ambient VOC and NO_x concentrations as the "baseline" from which changes were calculated on a daily basis. The rationale is as follows: first, there is no ambient air quality standard for VOC, and second the NO_x air quality in 2004 (see Fig. 4) met the air quality standard. Thus, while one can try to project improved VOC and/or NO_x air quality in a future year, say 2025, based upon an implementation plan, the degree of improvement is difficult to estimate since regional growth will likely reduce any gains due to emission control strategies. Also, because we used daily air quality data to predict ozone for a given day and there is no good way to predict the VOC and NO_x concentrations on a daily basis in a distant future year.

To estimate the typical changes in VOC and NO_x concentrations, the year 2004 meteorology was not used; instead, a typical meteorological year (TMY2) was used, which was extracted for the region statistically from 1961–1990 and is the most typical meteorology (TMY2, 2006). The TMY2 is a complete annual cycle of hourly meteorological data extracted from the 30-year period to represent a typical, rather than a worst-case, long-term meteorological condition in a specific region.

The choice of using 2004 initial VOC and NO_x concentrations in conjunction with the TMY2 meteorology as inputs to the regression model could be considered "inconsistent", i.e., in the sense that a high initial VOC and NO_x concentration level could have been used on a day with good ventilation (meteorology), however, running the analysis for an entire season averages out the impact of such occurrences.

Table 1
Hydrogen demand parameters and assumptions

Parameter and assumption	Value
City population in Sacramento (in 2000)	1.393 million
Vehicle ownership	0.8 vehicles/person
Vehicle miles traveled (VMT)	15,000 miles/year
Fuel economy of HFCV	60 miles/kg hydrogen
Hydrogen consumption	0.7 kg/vehicle/day
Hydrogen station size	3000 kg/day
Liquid truck capacity	3000 kg liquid hydrogen

3.2. Hydrogen demand and supply

We assume that in Sacramento County, California, the current light duty gasoline-fueled fleet is held constant and still on the road in the same numbers, whereas additional HFCVs have been introduced and are operating at market penetrations of 9% and 20%, respectively. Thus, the total vehicle population is the sum of the current light duty fleet and added hydrogen vehicles. Table 1 shows hydrogen demand parameters and assumptions for Sacramento and Table 2 shows estimated hydrogen demand for regional vehicle use.

We assume that in a steady state, the hydrogen demand meets the hydrogen supply on a daily basis. To meet the hydrogen demand, three hypothetical hydrogen supply pathways are considered in this study: on-site hydrogen production, central hydrogen production with pipeline delivery systems, and

central hydrogen production with liquid hydrogen truck delivery systems. These supply pathways are chosen, as they are likely to be the lowest cost near-term supplies for hydrogen over the next few decades (NRC, 2004). The spatial layout of the hypothetical stations and hydrogen plant is shown in Figs. 1 and 2. For more details see Wang et al. (2007).

Table 2
Regional hydrogen demand for vehicle use

	Scenario 1	Scenario 2
HFCV market penetration	9%	20%
Number of HFCVs	111,400	278,600
Hydrogen fuel demand	78,000 kg/day	195,000 kg/day
Number of hydrogen stations	27	66

3.3. Life cycle emissions and incremental precursor pollution

The life cycle emissions of ozone precursors associated with each hydrogen pathway should be

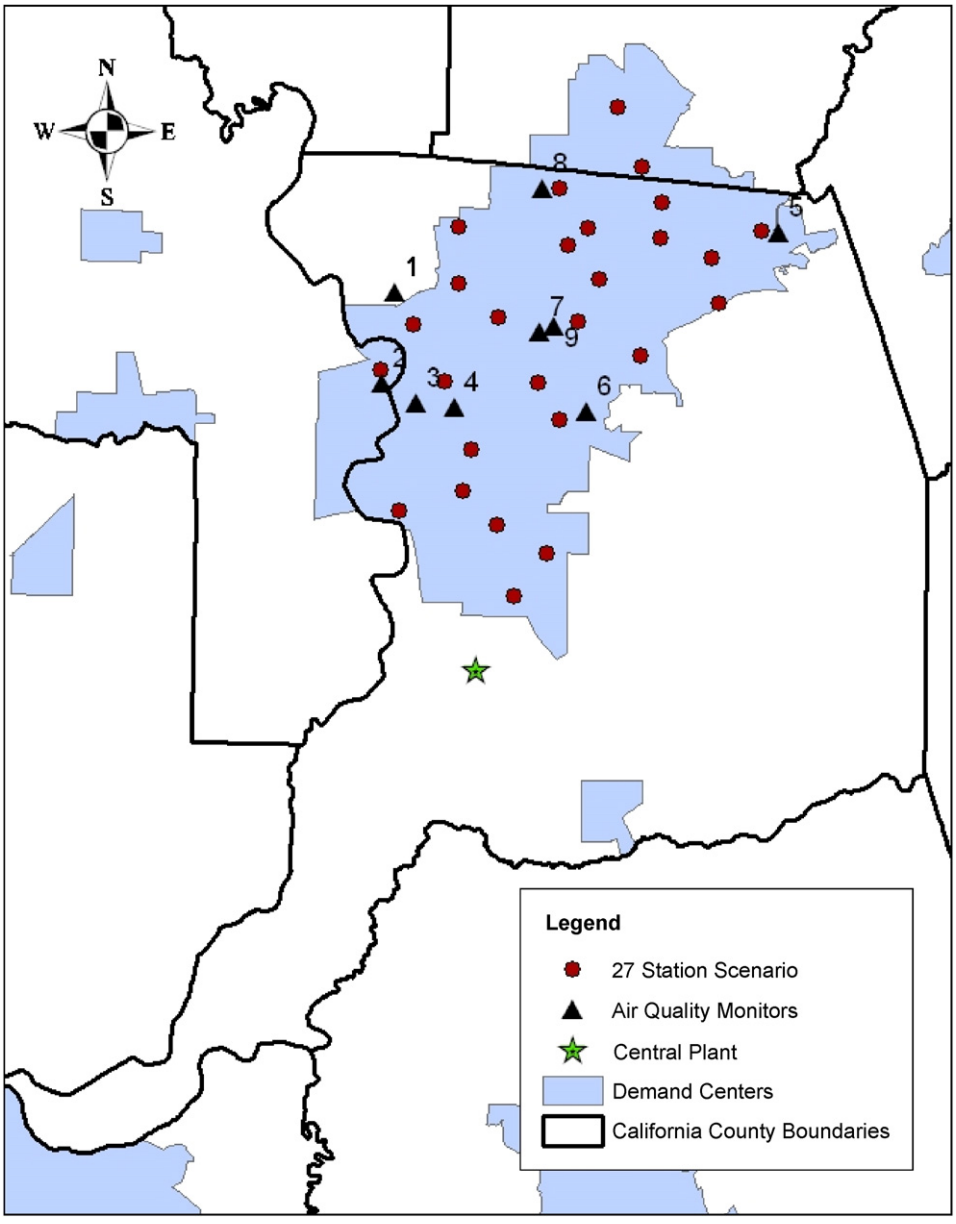

Fig. 1. Spatial layout of refueling stations, central plant, and receptors (9% scenario) (Wang et al., 2007).

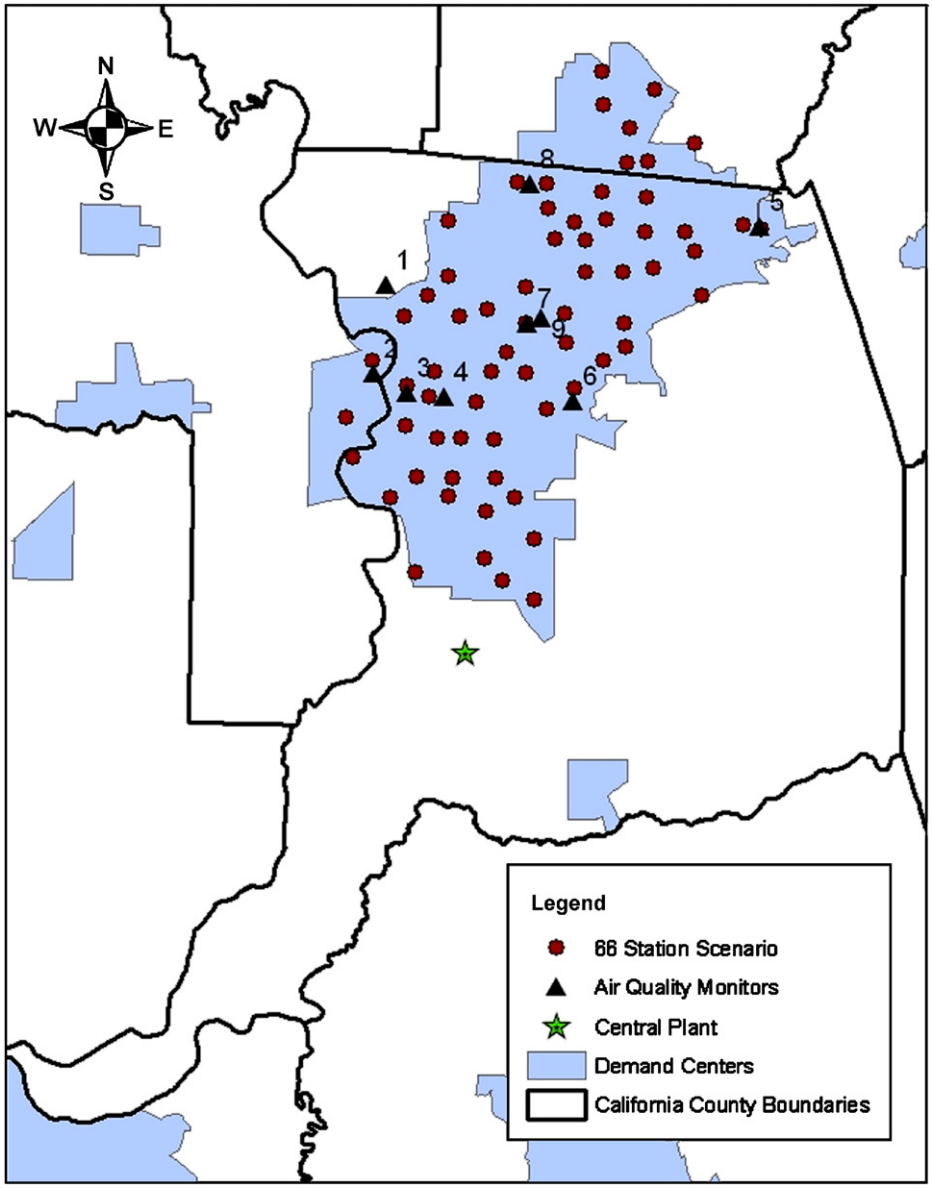

Fig. 2. Spatial layout of refueling stations, central plant, and receptors (20% scenario) (Wang et al., 2007).

used to determine the impact on ozone production. Life cycle emissions include all the emissions involved in producing and delivering hydrogen to vehicles, as well as emissions from electricity generation (for hydrogen compression) and petroleum use (diesel fuel for hydrogen truck delivery). Fig. 3 presents the life cycle of one of the three integrated NG to hydrogen pathways considered and the parts of the life cycle system included in this analysis are enclosed by the dashed line (Wang and Delucchi, 2005). The parts of the system outside the dashed line are assumed to be remote enough not to affect air quality in Sacramento. Emission factors are extracted from the GREET model (GREET1.7, 2006).

The emission inventories and spatial locations of emission sources have a strong influence on regional air quality. In this research, particular spatial locations for each step of a hydrogen supply pathway are assumed. Table 3 presents hydrogen pathway steps, locations, and emission inventories, as also described below.

(1) *Natural gas extraction and transport*: NG fields are located far away from Sacramento, and

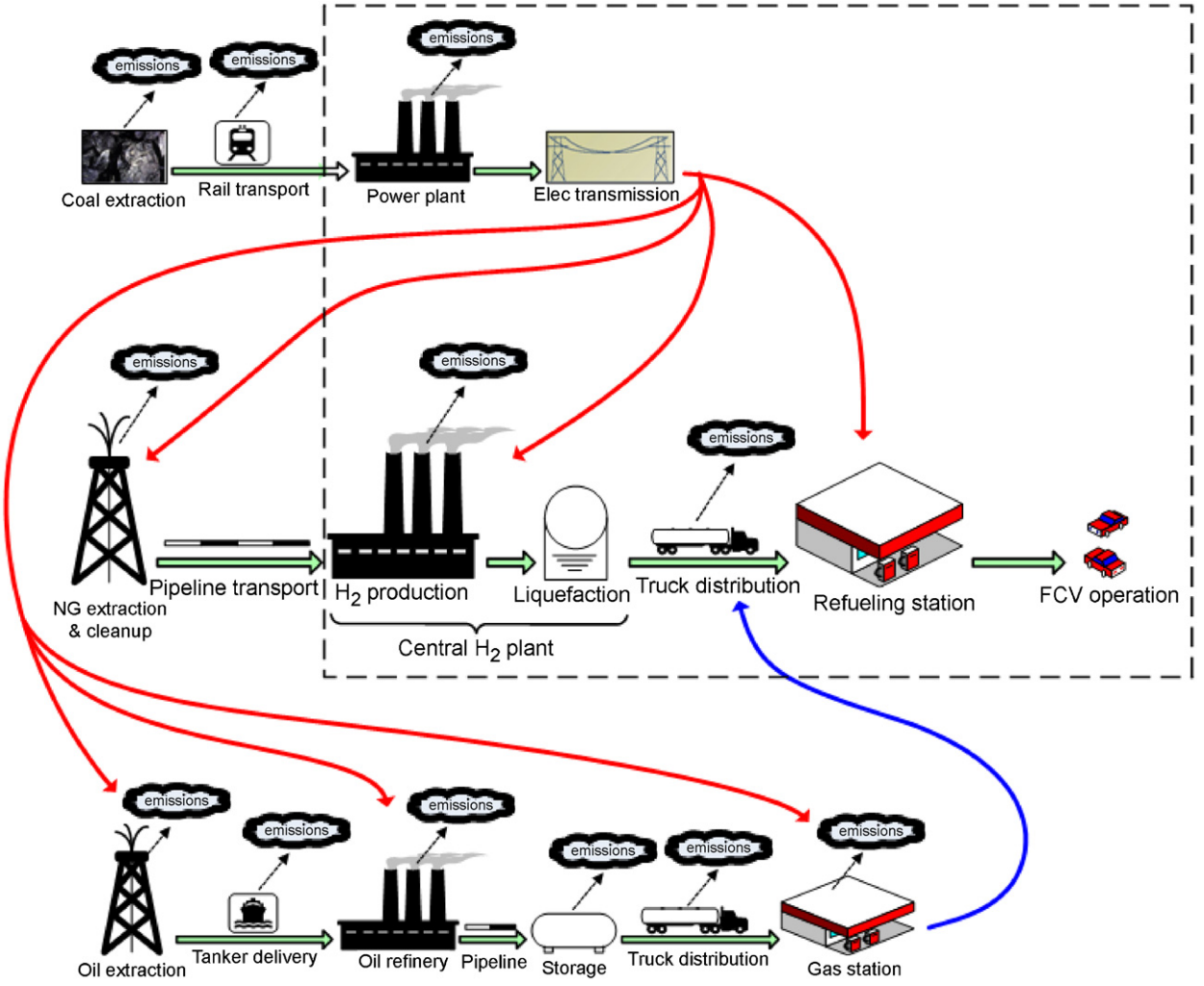

Fig. 3. Integrated NG-to-H_2 pathway (liquid hydrogen).

Table 3
Hydrogen pathway steps, locations, and emission inventories

Hydrogen pathways	Pathway steps included in the research
On-site hydrogen production	3,7,8,9 In this case, steps 3 and 7 are the same
Central hydrogen production with pipeline delivery systems	2,5,7,8,9
Central hydrogen production with liquid hydrogen truck delivery systems	2,4,6,7,8,9

therefore the impacts of NG extraction and pipeline transport on air quality in urban Sacramento are neglected. Thus, this pathway step is not included in the research on air quality.

(2) *Centralized hydrogen production*: Because of the availability of the NG, a central hydrogen production plant is assumed to be close to currently existing NG fired power plants in south Sacramento (see Figs. 1 and 2), and is treated as a point source of emissions.

(3) *On-site hydrogen production stations*: Emissions associated with hydrogen production from small steam reformers at refueling stations occur at the station sites. They are assumed to be a point source of emissions.

(4) *Electricity for hydrogen liquefaction*: Actual locations of utility plants in the Sacramento area are used to estimate incremental emissions associated with hydrogen liquefaction at the hydrogen plant. Although electricity is consumed at the central plant, the locations of

emissions occur at those utility plants which are assumed to be a point source.

(5) *Electricity for hydrogen compression at the central plant and pipeline delivery*: It is similar to electricity use for hydrogen liquefaction.
(6) *Liquid hydrogen truck delivery*: The actual route that each liquid hydrogen truck (from the central hydrogen plant to the station) travels is determined using GIS data on a minimum travel time basis. At the steady state, the road segments of the truck routes are treated as a thin-and-long area source of emissions.
(7) *Refueling stations*: Hydrogen station sites are selected from among existing gasoline station locations in Sacramento to minimize the average travel time from home to the closest station for all customers, given a certain number of stations (see Figs. 1 and 2). They are assumed to be a point source of emissions.
(8) *Electricity for hydrogen compression at refueling stations*: It is similar to electricity use for hydrogen liquefaction.
(9) *Vehicle operation*: Hydrogen vehicles are assumed not to emit any air pollutants examined in the research during operation, so their locations are not important for the analysis.

Based on the life cycle emission inventories and location information, a Gaussian dispersion model ISCST3 is run (ISCST3, 2006), together with TMY2 data for the region as the meteorological inputs to the model. The Typical Meteorological Year 2 (TMY2) is a complete annual cycle of hourly meteorological data extracted from the 30-year period of 1961–1990 to represent a typical, rather than a worst-case, long-term meteorological condition in a specific region (TMY2, 2006); therefore, the typical incremental concentrations of ozone precursors at each receptor (i.e., the air quality monitoring stations, shown in Figs. 1 and 2) due to atmospheric transport of emissions associated with hydrogen pathways could be determined. The incremental VOC and NO_x concentrations are then added to the baseline VOC and NO_x concentrations and used to estimate subsequent ozone formation, though not necessarily in proximity to the origin of the emissions.

3.4. Data and the ozone regression model

The air quality data used in this research are selected from the Air Quality System (AQS), which is maintained by US EPA and also contains profiles of many air quality monitoring stations throughout the country (AQS, 2006). However, the data on VOC and ozone are not complete for the year 2004. Even though more than 10 air quality monitoring stations were operating in Sacramento County in 2004, only one of them (see station 9 shown in Figs. 1 and 2) has relatively good-quality VOC data available. The prevailing wind in the region is commonly in the direction from southwest to northeast in the summer months, therefore station 5 is very often downwind of station 9, and it makes sense to assume that the early morning (say, 6:00 to 9:00 am) pollution level at station 9 provides the initial VOC and NO_x concentrations that form ozone that reach a maximum at the downwind station 5 (see Figs. 1 and 2). This paper uses data for 93 days in the summer (most of the period July 3, 2004 through October 26, 2004), the season during which ozone pollution mainly occurs.

An intrinsically linear regression model is developed to explore the relationship of ozone formation specific to the region. Consider initially that the peak ozone concentration is related to a number of factors, shown as

$$O_3(\max) = f(\mathrm{VOC},\ NO_x,\ \mathrm{Temp(max)},\ \mathrm{RH(avg)},\ \text{Solar radiation},\ \text{Wind speed},\ \text{etc.}), \quad (1)$$

where f represents a certain functional relationship; O_3(max), the peak ozone concentration ultimately reached (i.e., 1-h maximum ozone concentration of day) at the receptor station 5 (representing a station downwind of the urban area and often reflecting the maximum ozone pollution level observed in Sacramento), in units of parts per billion (ppb); VOC (or NO_x), the initial ambient VOC (or NO_x) concentration at air quality monitoring station 9 (representing a typical central urban Sacramento pollution level). They are the 3-h average of the ambient VOC (or NO_x) concentrations between 6:00 and 9:00 am, in units of ppb C (or ppb); Temp(max), the 1-h maximum temperature of day, °C; and RH(avg), the daily average relative humidity, %.

Using regression analysis, only four factors, namely the initial VOC concentration, the initial NO_x concentration, the maximum hourly temperature of day, and the daily average relative humidity, are observed to be statistically significant and theoretically meaningful, and are therefore selected. The initial ambient VOC, the initial ambient NO_x,

and the observed ambient peak ozone during the period of regression are shown in Fig. 4, and the meteorological conditions used in the regression are shown in Fig. 5.

The following regression model (or equation) is estimated with ordinary least squares (OLS) and ascertained to best correspond to all the groups of air quality data (see Eq. (2)).

The regression coefficient of determination is $R^2 = 0.65$, and the sample size is $N = 93$. The numbers in parentheses under the equation are t-statistics for the corresponding regression coefficients. The Durbin–Watson test gives DW = 1.580, which provides no evidence of the existence of auto correlation in the model specification using the time series data.

$$O_3(\max) = -54.268 + 3.069\ \mathrm{Temp(max)} + 0.406\ \mathrm{RH(avg)} + 0.474\ NO_x - 0.521\ NO_x^2/\mathrm{VOC}$$
$$(-2.644)\quad (7.628)\qquad (2.478)\qquad (2.376)\qquad (-2.017). \tag{2}$$

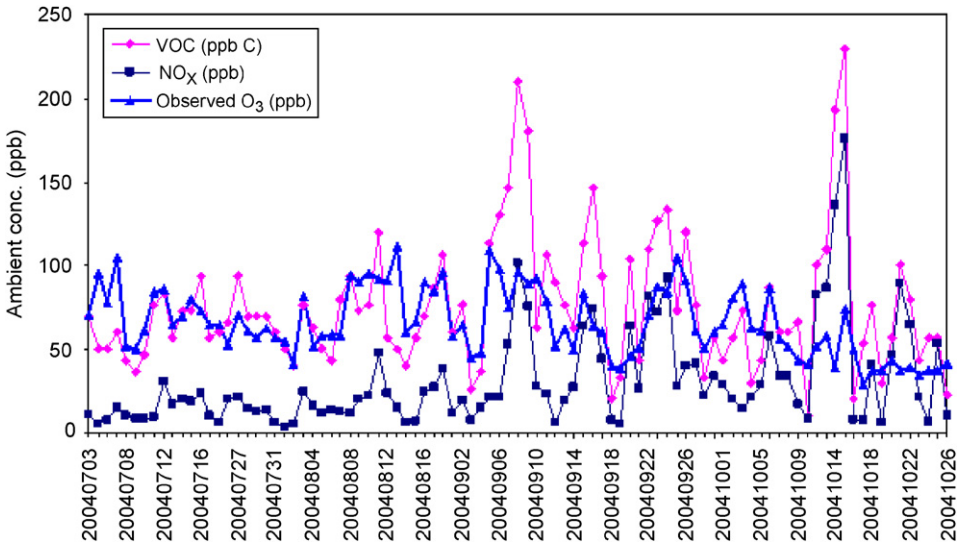

Fig. 4. Actual ambient concentrations of pollutants used in the regression.

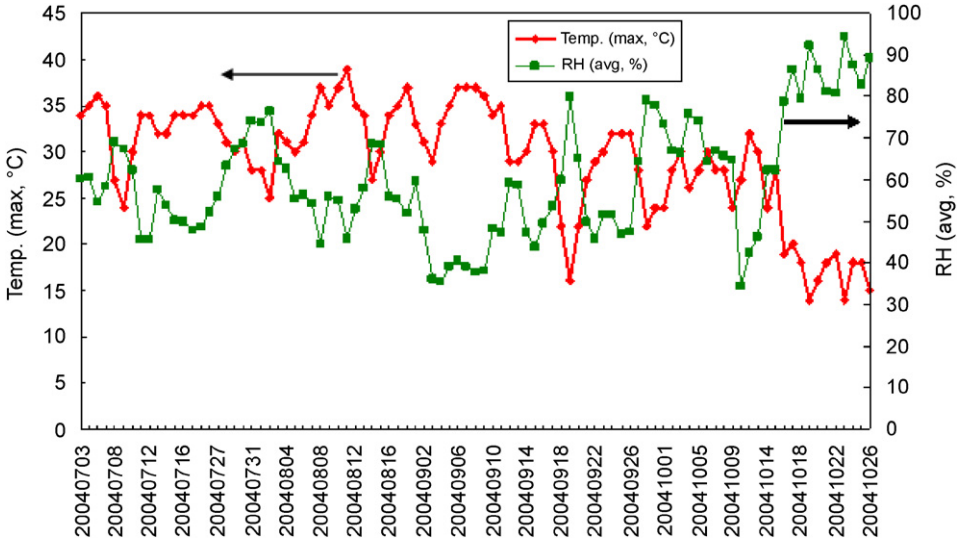

Fig. 5. Actual meteorological conditions used in the regression.

The regression is limited to the training data set and hence to the corresponding region and time period. The explanatory variable, Temp(max), is extremely important, and its coefficient is significantly different from zero (t-statistic is 7.628). The temperature effect is correlated with sunlight as well as other meteorological conditions associated with the build-up of pollutants, e.g., low wind speed, so it is possible that several meteorological factors are included in Temp(max). However, the effect of RH may not be partially captured in Temp(max) because model hypothesis testing and auxiliary regressions have not identified collinearity between Temp(max) and RH(avg) for this training data set even though RH is, in general, inversely related to temperature.

Based on the standard ozone isopleth diagram produced by EKMA, there can be divergent predictions of ozone formation (increment or decrement) depending, to some extent, on the ambient ratio of initial VOC to NO_x as the concentration of NO_x increases. This is reflected by the regressor NO_x^2/VOC, which is equal to the NO_x concentration divided by the ratio of VOC to NO_x. The ratios for the training data set happen to be within $0 < VOC/NO_x \leqslant 20$ (see Fig. 6). There is no case in which the ratio VOC/NO_x is greater than 20 in the data set of the research, so the regression equation should perhaps not be applied to situations where $VOC/NO_x > 20$. Intuitively, the functional relationship where $VOC/NO_x > 20$ is very likely to be, or be close to, a straight line parallel to the VOC axis based on a standard EKMA ozone isopleth diagram when plotted in terms of initial VOC and NO_x (NRC, 1991).

The comparison of the observed and predicted peak ozone concentrations at receptor station 5 are shown in Fig. 7. Even though the prevailing wind commonly blows from southwest to northeast in the summer, due to the wind speed/direction variability the geographical location where peak ozone concentrations occur may differ from receptor station 5 (as can be observed from photochemical grid model simulations), and thus the predicted concentration at station 5 is simply an approximation of the observed or theoretical concentration derived from smog chamber experiments or chemical reaction mechanisms. That in part explains why R^2 is not higher in the regression; that is, about 65% of the variation in peak ozone concentrations can be accounted for by the regression variables selected, but they cannot account for the day-specific variation of spatial transport of the predicted emissions to receptor 9 by the ISCST3 model or of subsequent ozone formed by those emissions to receptor 5.

3.5. Applying the regression model

Three hydrogen supply pathways are considered, and for each of them there are two sets of market penetrations 9% and 20%. Therefore, there are a total of six scenarios. Based on a previous study

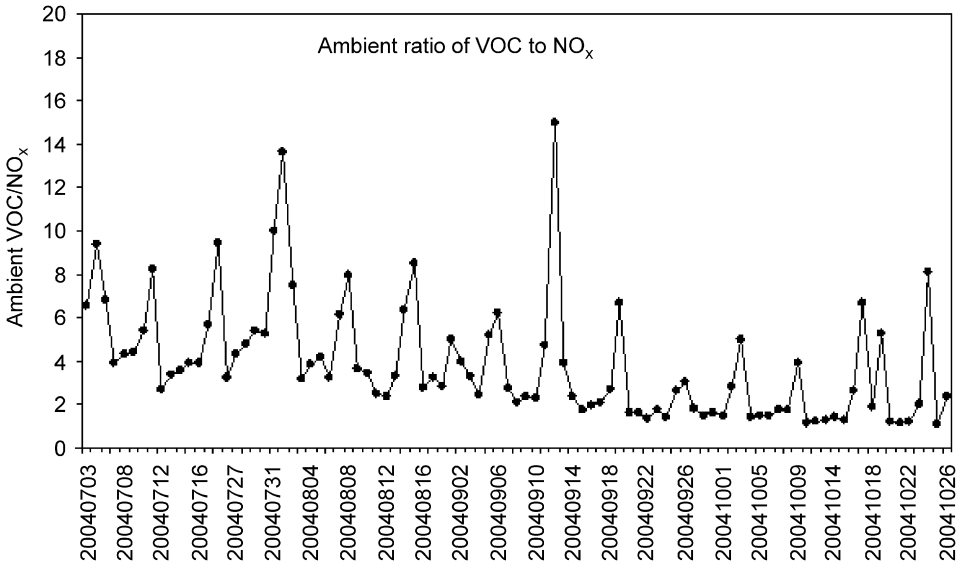

Fig. 6. Ambient ratio of VOC to NO_x at station 9.

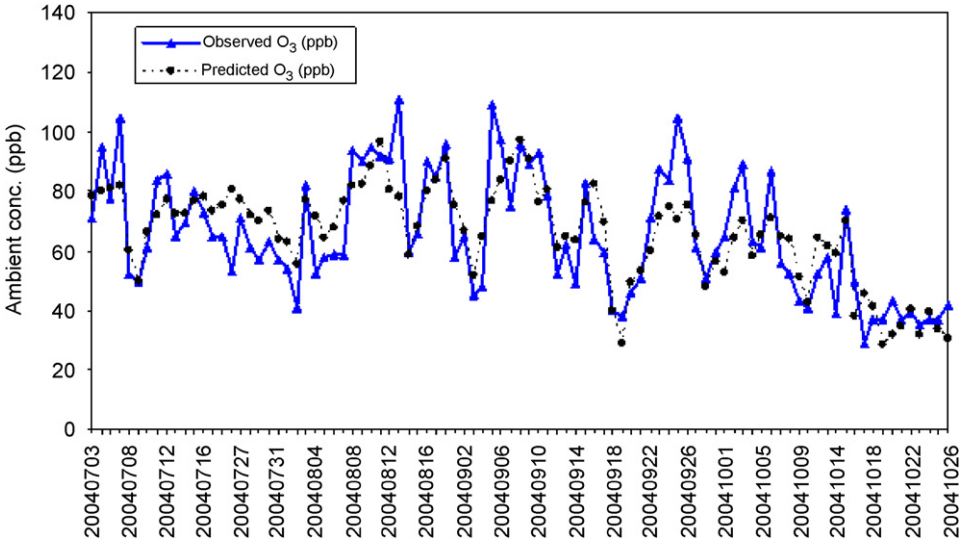

Fig. 7. Comparison of the observed and predicted peak ozone concentrations.

(Wang et al., 2007), the changes in ambient concentrations of primary pollutants, including VOC and NO_x, at monitoring stations have been determined. Below are the steps to estimate the changes in ozone air quality due to life cycle emissions of each hydrogen pathway.

(1) Estimate the incremental VOC and NO_x concentrations (i.e., the 3-h average of 6:00–9:00 am or the daily average, at station 9), caused by atmospheric physical transport and associated with each of six hydrogen supply scenarios. This step is accomplished using atmospheric dispersion models along with typical meteorological year data. No atmospheric chemical transformation is considered and only directly emitted primary pollutants are investigated for this step; therefore, secondary ozone pollution has not been included up to this point in the analysis. For more details see Wang et al. (2007). The percentage change in VOC or NO_x is expressed as

$$\%\Delta\mathrm{VOC} = \frac{\text{new VOC} - \text{baseline VOC}}{\text{baseline VOC}} \times 100\% = \frac{\text{incremental VOC}}{\text{baseline VOC}} \times 100\%, \quad (3)$$

$$\%\Delta\mathrm{NO}_x = \frac{\text{new NO}_x - \text{baseline NO}_x}{\text{baseline NO}_x} \times 100\% = \frac{\text{incremental NO}_x}{\text{baseline NO}_x} \times 100\%. \quad (4)$$

(2) Add the incremental VOC and NO_x to the baseline VOC and NO_x concentrations (i.e., the current ambient background VOC and NO_x in 2004), and use the sum as inputs to the ozone-and-precursor regression model developed in this paper (see Eq. (2)).

(3) Calculate the new peak ozone concentrations day by day using the same meteorological data as in the regression model. The calculated results are for station 5 (see Figs. 1 and 2).

(4) Compute the difference between the new ozone and the previously predicted ozone that is estimated using ambient background VOC and NO_x as inputs to the regression model. Now, the changes in ozone air quality, denoted by $\Delta O_3(\max)$, and the percentage changes in ozone levels, denoted by $\%\Delta O_3(\max)$, associated with a hydrogen pathway can be determined. Below are the formulas (see Eqs. (5) and (6)).

$$\Delta O_3(\max) = \text{new } O_3(\max) - \text{baseline } O_3(\max), \quad (5)$$

$$\%\Delta O_3(\max) = \frac{\text{new } O_3(\max) - \text{baseline } O_3(\max)}{\text{baseline } O_3(\max)} \times 100\%. \quad (6)$$

Note that the changes in initial VOC and NO_x are small relative to the baseline pollution level, so it

makes sense to apply the regression model to these "new" input data since they remain within the range of observations in the region.

4. Results and discussion

4.1. Incremental 3-h average pollution of ozone precursors

The incremental 3-h average concentrations of VOC and NO_x at station 9 are shown in Tables 4 and 5. Those numbers are additional pollution, caused by life cycle emissions from six hypothetical hydrogen pathways, respectively, and occurring at station 9, which subsequently results in ozone pollution at station 5 commonly downwind of station 9. Relative to the actual ambient pollution level at station 9, Figs. 8–11 compare the incremental 3-h average pollution of physically transported VOC and NO_x associated with each hydrogen pathway.

At the 9% market penetration, the on-site pathway causes additional VOC concentrations of 0–0.007%, the pipeline pathway causes 0–0.014% (there is an outlier 0.041%), and both are much smaller than the truck pathway that causes additional VOC concentrations of 0–0.027%. At the 20% market penetration, the on-site pathway causes additional VOC concentrations of 0–0.058%, the pipeline pathway causes 0–0.034% (again, there is an outlier 0.102%), and the truck pathway causes additional VOC concentrations of 0–0.067%.

At the 9% market penetration, the on-site pathway causes additional NO_x concentrations of 0–0.140%, the pipeline pathway causes 0–0.381% (an outlier is 0.795%), and the truck pathway results in additional NO_x concentrations of 0–0.750%. At the 20% market penetration, the on-site pathway causes additional NO_x concentrations of 0–0.443%, the pipeline pathway causes 0–0.952% (the outlier is 1.987%), and the truck pathway results in additional NO_x concentrations of 0–1.861%.

In conclusion, the truck pathways have the greatest impact on both VOC and NO_x pollution, the on-site pathways have a smallest impact, and the pipeline pathways are between them (even though the pipeline pathways and the on-site pathways are almost comparable in terms of the resulting additional VOC or NO_x pollution). Particularly, the real-world NO_x pollution at station 9 was often relatively low in 2004 (see Fig. 4), and diesel hydrogen-delivery trucks emit substantial amounts of NO_x, which explains why the truck pathway at the 20% market penetration can lead to up to a 2% increase of the current NO_x pollution levels.

Table 4
Descriptive statistics on incremental 3-h average VOC concentrations, ppb C

Scenario	*N*	Range	Minimum	Maximum	Mean	Std. deviation
On-site, 27	93	0.00398	0.00000	0.00398	0.00066	0.00074
Pipeline, 27	93	0.00817	0.00000	0.00817	0.00080	0.00164
Truck, 27	93	0.01479	0.00000	0.01479	0.00206	0.00301
On-site, 66	93	0.03617	0.00000	0.03617	0.00282	0.00487
Pipeline, 66	93	0.02043	0.00000	0.02043	0.00200	0.00410
Truck, 66	93	0.03689	0.00000	0.03689	0.00520	0.00748

Table 5
Descriptive statistics on incremental 3-h average NO_x concentrations, ppb

Scenario	*N*	Range	Minimum	Maximum	Mean	Std. deviation
On-site, 27	93	0.02015	0.00000	0.02015	0.00299	0.00330
Pipeline, 27	93	0.06097	0.00000	0.06097	0.00516	0.01089
Truck, 27	93	0.07298	0.00000	0.07298	0.01063	0.01588
On-site, 66	93	0.18763	0.00000	0.18763	0.01369	0.02490
Pipeline, 66	93	0.15242	0.00000	0.15242	0.01290	0.02721
Truck, 66	93	0.18194	0.00000	0.18194	0.02686	0.03932

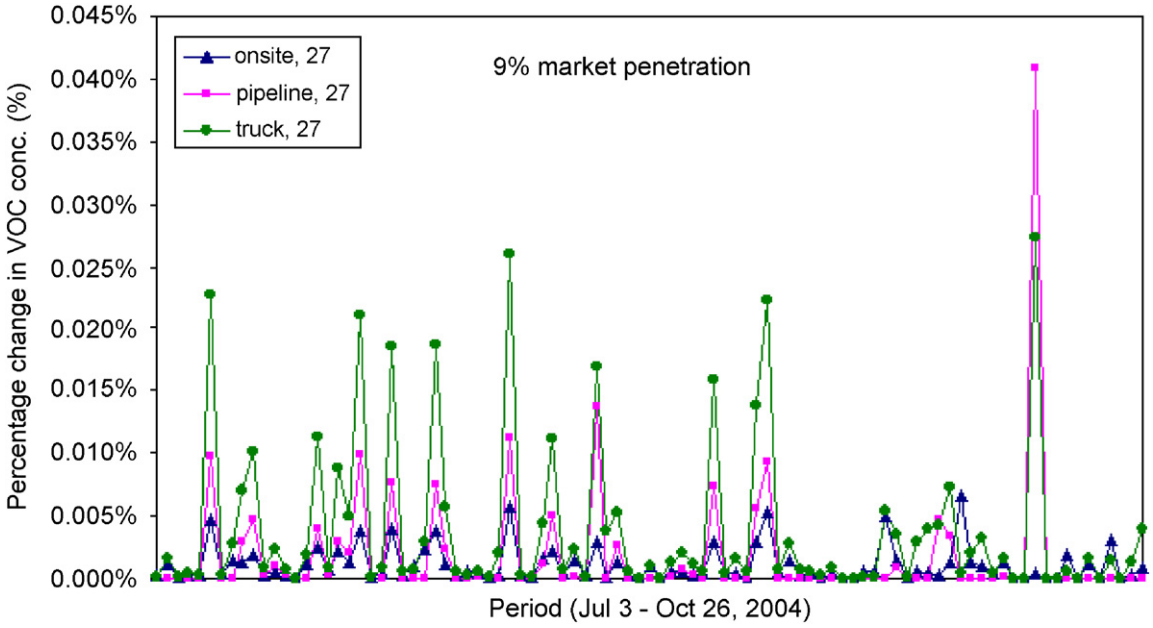

Fig. 8. Comparison of percentage changes in 3-h average VOC concentrations (9% market penetration).

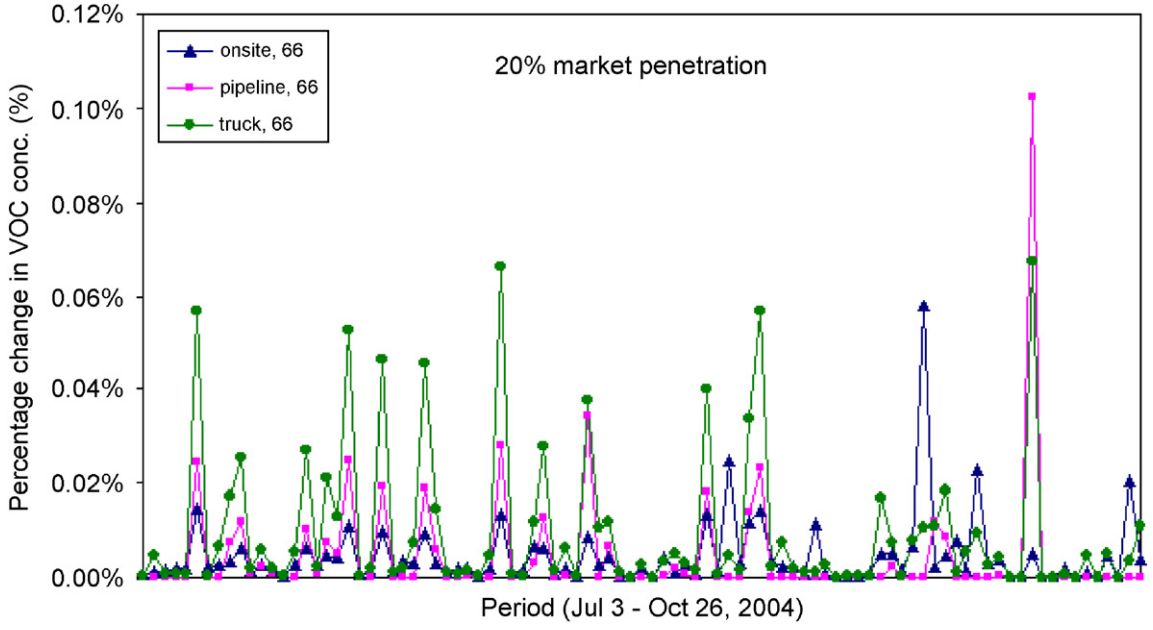

Fig. 9. Comparison of percentage changes in 3-h average VOC concentrations (20% market penetration).

4.2. *Changes in peak ozone concentrations, $\Delta O_3(max)$*

Ozone formation in the atmosphere is a complicated issue. Table 6 summarizes the estimated changes in 1-h peak ozone concentrations due to life cycle emissions of each hydrogen pathway. The range of ΔO_3(max) results increases as the market penetrations increase from 9% (corresponding to 27 refueling stations) to 20% (corresponding to 66 refueling stations). At the same market penetration, truck pathways correspond to the widest range of

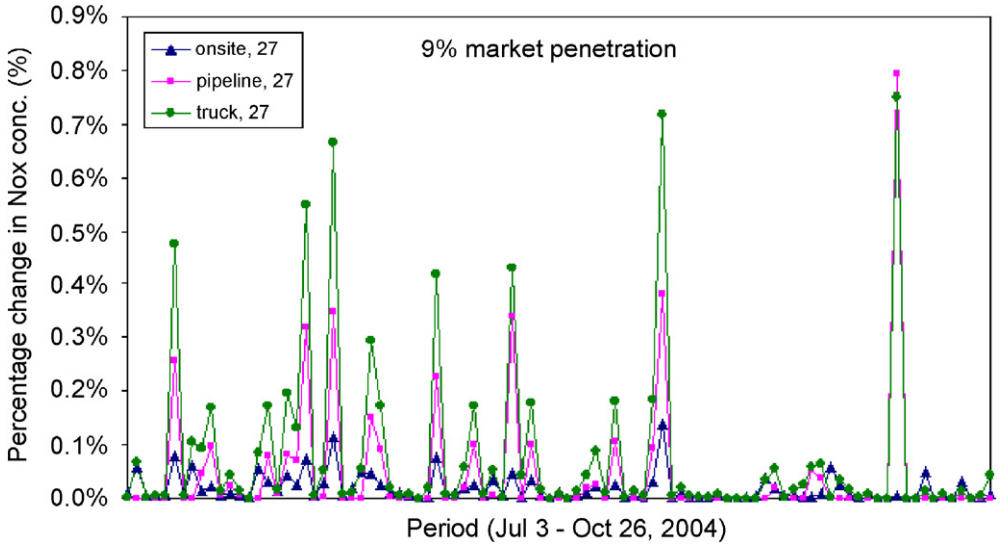

Fig. 10. Comparison of percentage changes in 3-h average NO_x concentrations (9% market penetration).

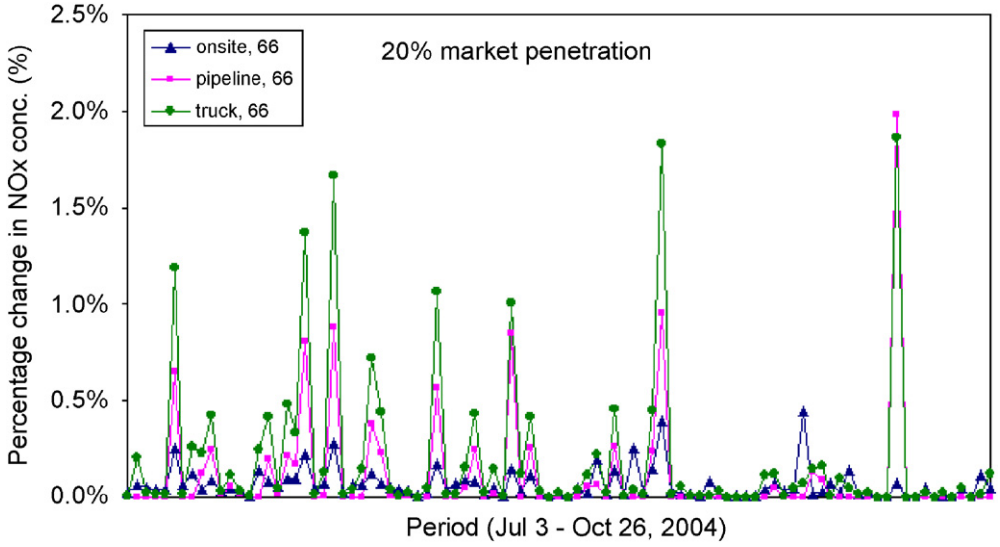

Fig. 11. Comparison of percentage changes in 3-h average NO_x concentrations (20% market penetration).

Table 6
Descriptive statistics on changes in peak ozone concentrations, ΔO_3(max), ppb

Scenario	*N*	Range	Minimum	Maximum	Mean	Median	Std. deviation
On-site, 27	93	0.00512	−0.00237	0.00275	0.00031	0.00019	0.00083
Pipeline, 27	93	0.01761	−0.00574	0.01187	0.00081	0.00000	0.00213
Truck, 27	93	0.02684	−0.00648	0.02036	0.00155	0.00018	0.00371
On-site, 66	93	0.03351	−0.02523	0.00828	0.00016	0.00084	0.00472
Pipeline, 66	93	0.04401	−0.01437	0.02964	0.00201	0.00000	0.00530
Truck, 66	93	0.06702	−0.01641	0.05061	0.00377	0.00046	0.00926

ΔO_3(max) results, which means that truck pathways tend to result in much more variation in degradation or improvement of ozone air quality.

All the minimum ΔO_3(max) results are negative and all the maximum ΔO_3(max) results are positive, shown in Table 6, which means that increases in

initial VOC and NO_x concentrations do not necessarily increase the peak O_3 concentration, and may even result in a decrease. That is consistent with a standard EKMA ozone isopleth (NRC, 1991). Accounting for the meteorological conditions, this phenomenon depends on the ambient ratio of initial VOC and NO_x, i.e., relative abundance of initial VOC and NO_x. NO_x is relatively abundant in the NO_x-rich zone (or so-called "VOC-limited" zone) on a typical ozone isopleth diagram, which corresponds to the situations where VOC/NO_x is generally less than 7–10 (Chang et al., 1989; NRC, 1991). However, VOC is relatively abundant in the VOC-rich zone (or so-called "NO_x-limited" zone) on an ozone isopleth diagram, which corresponds to the situations where VOC/NO_x is generally greater than 7–10 (Chang et al., 1989; NRC, 1991).

4.3. Percentage changes in peak ozone concentrations, $\%\Delta O_3(max)$

Fig. 12 presents the comparison of $\%\Delta O_3$(max) results associated with these three hydrogen supply pathways. For the 9% market penetration, the on-site pathway causes $\%\Delta O_3$(max) within the range of −0.007% to 0.008%, and the pipeline pathway causes $\%\Delta O_3$(max) within the range of −0.008% to 0.021%. The truck pathway causes $\%\Delta O_3$(max) within the range of −0.009% to 0.039% which is wider than the on-site and pipeline pathways.

For the 20% market penetration, the on-site pathway causes $\%\Delta O_3$(max) within the range of −0.075% to 0.022%, and the pipeline pathway causes $\%\Delta O_3$(max) within the range of −0.020% to 0.052%, shown in Fig. 13. Moreover, Fig. 13 also demonstrates that the truck pathway causes $\%\Delta O_3$(max) within the range of −0.023% to 0.100%, which is wider than the on-site and pipeline pathways as well.

During the modeling period (July 3, 2004 through October 26, 2004), two obviously different ozone pollution trends appear. One occurs in the days preceding September 15, 2004, when the incremental VOC and NO_x from hydrogen pathways typically lead to an increase in the ozone level, and the resulting ozone pollution goes up in the following order: the on-site pathway, the pipeline pathway, and the truck pathway. That is, during the worst summer months for ozone pollution, July, August, and September, the changes in $\%\Delta O_3$(max) are almost all positive, therefore a worsening of ozone air quality would occur. The other trend occurs after September 15 (mostly in October), and all pathways often lead to no ozone pollution or even a decrease in ozone formation; especially

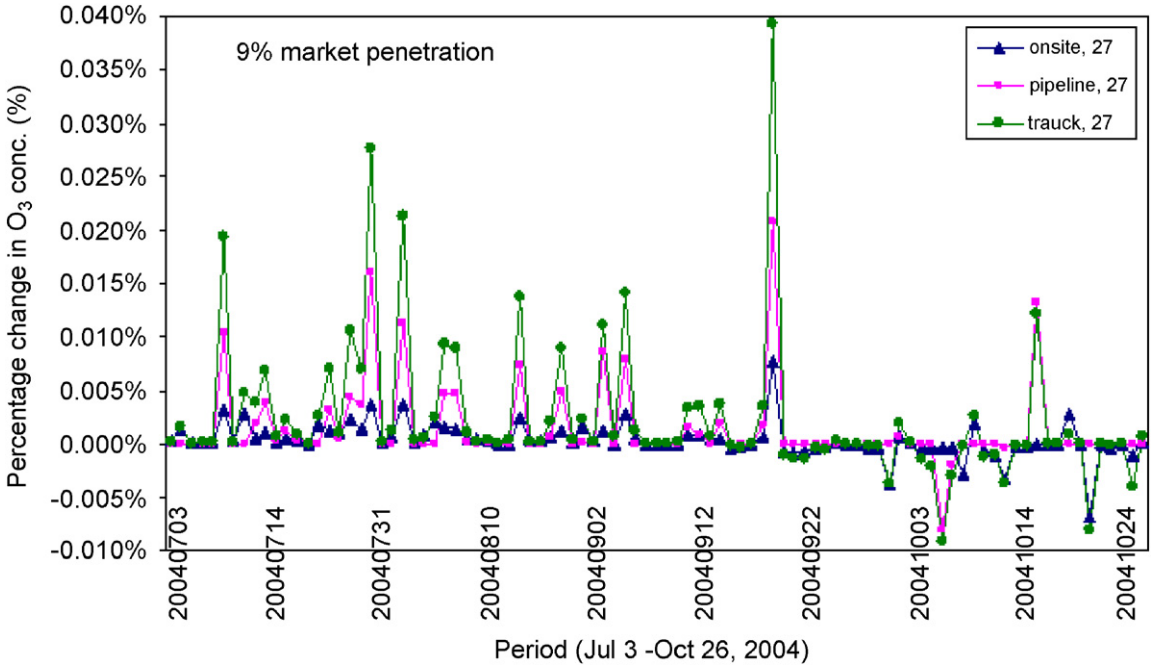

Fig. 12. Comparison of percentage changes in peak ozone concentrations (9% market penetration).

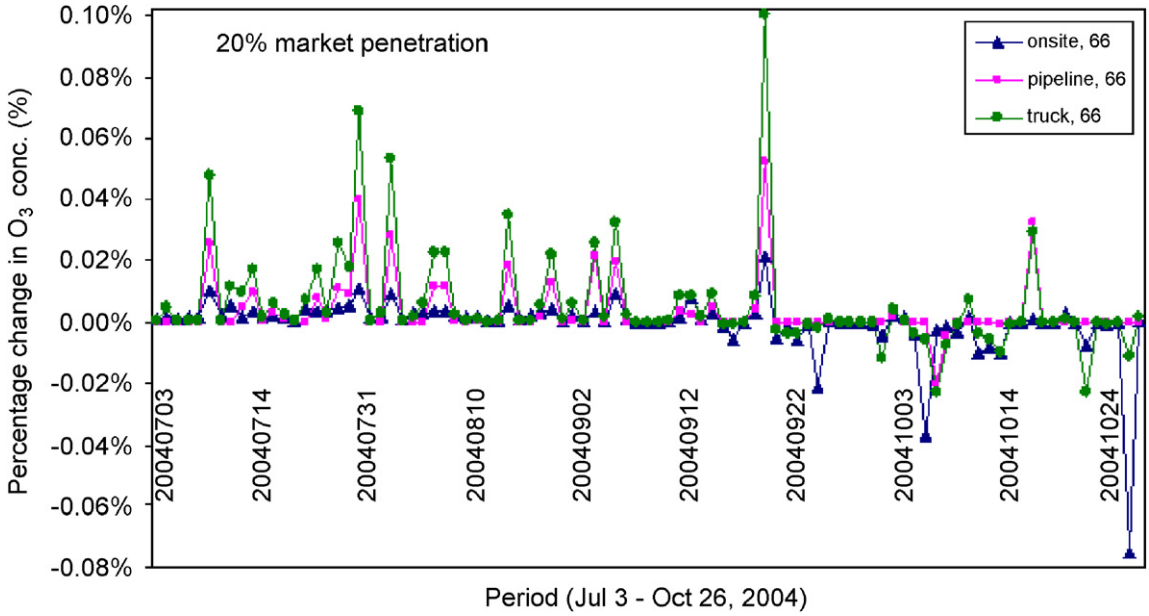

Fig. 13. Comparison of percentage changes in peak ozone concentrations (20% market penetration).

on-site and truck pathways lead to greater decreases in ozone pollution.

At the 20% market penetration, the greatest increase can be up to 0.1% of the current ozone level (corresponding to the truck pathway), and the greatest decrease can be around −0.1% of background ozone pollution (corresponding to the on-site pathway). In summary, all the pathways result in very small changes in ozone air quality. However, Figs. 12 and 13 both show that the truck pathway causes $\%\Delta O_3(max)$ to fluctuate much more than do the other two hydrogen pathways (especially in July, August, and September). Therefore, just in terms of ozone pollution, all the three hydrogen pathways in some cases would result in a better ozone air quality, corresponding to a negative $\%\Delta O_3(max)$, and in some cases will result in a worse ozone air quality, corresponding to a positive $\%\Delta O_3(max)$, but there is little doubt that the truck pathway tends to lead to a much wider fluctuation in degradation or improvement of ozone air quality.

4.4. Further discussion on ozone pollution

The ozone pollution caused by the truck pathways are most widely fluctuating; percentage changes in peak ozone concentrations are approximately −0.01% to 0.04% for the 9% market penetration, and approximately −0.03% to 0.1% for the 20% market penetration. Note that the 20% on-site pathway sometimes can cause a decrease around −0.1% of background ozone pollution. The federal ozone standard is 80 ppb within the 8-h averaging time (NAAQS, 2006), and the California ozone standard is 70 ppb within the 8-h averaging time and 90 ppb within the 1-h averaging time (CARB, 2006). Figs. 4 and 7 shows that California 1-h ozone standard is violated on some days during the modeling period, but the ambient peak ozone is often in the vicinity of the standard. Therefore, the truck pathways (and the on-site and pipeline pathways) are unlikely to lead to a serious ozone problem in Sacramento.

Since the same meteorological conditions for each day are used when deriving the regression model and applying the model to the analysis of hydrogen supply scenarios, the changes in peak ozone concentrations shown in Figs. 12 and 13 are due only to the variation in VOC and NO_x inputs to the model. Most of the largest positive peaks in $\%\Delta O_3(max)$ in the summer (before September 15, 2004) correspond to the lowest VOC/NO_x ratios on those days, about 3.2–5.2 (see Figs. 6, 12 and 13). Because the estimate of the ratios of the incremental VOC and the incremental NO_x due to a hydrogen supply pathway is about 0.1–0.3, the new VOC/NO_x ratios inputted to the model would decrease. That is, the VOC/NO_x ratio goes down and the peak ozone concentration goes up accordingly. In other words, VOC, NO_x, and peak O_3 concentrations are

all positive increases. Therefore, ozone formation is generally in the NO_x limited regime (limited by NO_x) in the summer in that part of Sacramento. On the contrary, most of the largest negative peaks in $\%\Delta O_3$(max) in the fall (after September 15, 2004) correspond to the lowest VOC/NO_x ratios, approximately 1.1–1.5 (see Figs. 6, 12 and 13). Similarly, the new VOC/NO_x ratios input to the model would decrease. That is, the VOC/NO_x ratio goes down and the resulting peak ozone concentration also goes down. Put another way, both VOC and NO_x increase, but peak O_3 concentrations decrease. Therefore, ozone formation mostly is limited by VOC in the fall. In summary, the ozone production ridge line on the isopleth corresponds to a VOC/NO_x ratio between 1.5 and 5.2 in Sacramento, which is slightly lower than a typical EKMA value. That could be in part because the Sacramento region is not a closed smog chamber, station 5 is not always where peak ozone formation occurs due to the variability of wind speed and direction, and the statistical model parameters are only estimates.

5. Conclusions

We assumed two sets of hydrogen vehicle market penetrations 9% and 20%, respectively, and considered the following three hypothetical NG to hydrogen pathways in the research: on-site hydrogen production, central hydrogen production with gaseous hydrogen pipeline delivery, and central hydrogen production with liquid hydrogen truck delivery. Hydrogen was assumed to be produced by the process of steam reforming of NG, which is most commonly used today. Prior to estimating changes in ozone air quality due to each hydrogen pathway, life cycle emission inventories and optimized spatial layouts of hydrogen infrastructure were determined.

Atmospheric ozone formation is complicated. In the research, a region-specific linear regression model was developed to link the peak ozone concentrations to ambient meteorological conditions and the early morning ambient VOC and NO_x as the precursors to ozone formation. The regression model and data were limited to the Sacramento region and the time period from July 3, 2004 to October 26, 2004. The model shows that increases in precursor concentrations do not necessarily increase the peak ozone concentration, and may even cause it to decrease. The results indicate that, in Sacramento, ozone formation is generally limited by NO_x in the summer and is mostly limited by VOC in the fall. The ozone production ridge line on the isopleth corresponds to a VOC/NO_x ratio between 1.5 and 5.2 in Sacramento, which is slightly lower than typical values observed in a closed smog chamber and EKMA diagrams. The ozone monitoring station used in the regression analysis is also not always an accurate indicator of peak ozone formation due to the variability of wind speed and direction.

Considering only atmospheric transport of pollutants, truck pathways have the greatest impact on both VOC and NO_x pollution, the on-site pathways have a smallest impact, and the pipeline pathways are between them. Since the current light duty fleet is held constant and additional hydrogen cars are added to the fleet, the incremental VOC and NO_x pollution resulting from life cycle emissions of all hydrogen pathways is a positive quantity. At 9% market penetration, the truck pathway caused additional VOC (or NO_x) up to around 0.05% (or 1%) of current pollution level in 2004; at 20% market penetration, the truck pathway caused additional VOC (or NO_x) up to around 0.1% (or 2%) of current pollution level.

All the hydrogen pathways would result in very small (either negative or positive) changes in ozone air quality. In some cases worse ozone air quality (mostly in July, August, and September) resulted and ozone increments increased in the following order: the on-site pathway, the pipeline pathway, and the truck pathway. In some cases better ozone air quality was predicted to result (mostly in October), and the truck and on-site pathways had a greater impact than the pipeline pathway. The truck pathway tended to lead to a much wider fluctuation in degradation or improvement of ozone air quality: percentage changes in peak ozone concentrations are approximately -0.01% to 0.04% for the 9% market penetration, and approximately -0.03% to 0.1% for the 20% market penetration. Note that the 20% on-site pathway occasionally resulted in a decrease of around -0.1% of background ozone pollution. So the positive and negative limits of changes in ozone pollution would be around one thousandth of current pollution levels. Compared to the current ambient pollution level, the truck pathways (and the on-site and pipeline pathways) are unlikely to cause a serious ozone problem for market penetration levels of HFCVs in the 9–20% range.

The quantified ozone concentrations can be used to estimate agricultural losses and human health damages. Based on the predicted changes in ozone pollution (and other criteria pollutant concentrations), dose–response functions, and demographic data in Sacramento, social costs associated with hydrogen supply pathways can be estimated, which is useful for urban planners and policymakers.

Acknowledgments

The authors would like to thank the Hydrogen Pathways program at the Institute of Transportation Studies (ITS) at the University of California, Davis for its support.

The authors appreciate the information provided by Dwight Oda (California Air Resources Board), Dr. Christopher Yang (ITS, UC Davis) and Michael Nicholas (ITS, UC Davis). For useful comments, the authors also wish to acknowledge Professor Patricia Mokhtarian (Civil & Environmental Engineering, UC Davis).

References

AQS, 2006. Air Quality System. US EPA. 〈http://www.epa.gov/ttn/airs/airsaqs/detaildata/downloadaqsdata.htm〉. Accessed on 11/13/2006.

CARB, 2006. Ambient Air Quality Standards. California Air Resources Board. 〈http://www.arb.ca.gov/aqs/aaqs2.pdf〉. Accessed on 5/31/2006.

Chaaban, F.B., Nuwayhid, I., Djoundourian, S., 2001. A study of social and economic implications of mobile sources on air quality in Lebanon. Transportation Research Part D 6, 347–355.

Chang, T.Y., Rudy, S.J., Kuntasal, G., Gorse, R.A., 1989. Impact of methanol vehicles on ozone air quality. Atmospheric Environment 23, 1629–1644.

Delucchi, M., McCubbin, D., 2004. The contribution of motor vehicle and other sources to ambient air pollution. Report #16 in the series: The Annualized Social Cost of Motor-Vehicle Use in the United States, based on 1990–1991 Data. Publication No. UCD-ITS-RR-96-3 (16) rev. 1, Institute of Transportation Studies, University of California at Davis.

Delucchi, M., Murphy, J., McCubbin, D., Kim, J., 1998. The Cost of Crop Damage Caused by Ozone Air Pollution from Motor Vehicles. Research Report UCD-ITS-RR-96-03(12), Institute of Transportation Studies, University of California at Davis.

Derwent, R.G., Jenkin, M.E., Saunders, S.M., 1996. Photochemical ozone creation potentials for a large number of reactive hydrocarbons under European conditions. Atmospheric Environment 30, 181–199.

ExternE, 1998. Externalities of Energy, Methodology 1998 Update. European Commission. 〈http://www.externe.info/reportex/vol7.pdf〉. Accessed on 6/10/2005.

GREET1.7, 2006. The Greenhouse Gases, Regulated Emissions, and Energy Use in Transportation (GREET) Model. Argonne National Laboratory. 〈http://www.transportation.anl.gov/software/GREET/index.html〉. Accessed on 5/25/2006.

ISCST3, 2006. Industrial Source Complex model (Short Term 3). US EPA. 〈http://www.epa.gov/scram001/dispersion_alt.htm〉. Accessed on 5/25/2006.

Kelly, N.A., Gunst, R.F., 1990. Response of ozone to changes in hydrocarbon and nitrogen oxide concentrations in outdoor smog chambers with Los Angeles air. Atmospheric Environment 24A, 2991–3005.

Kinoslan, J.R., 1982. Ozone-precursor relationships from EKMA diagrams. Environmental Science and Technology 16, 880–883.

McCubbin, D., Delucchi, M., 1996. The Social Cost of the Health Effects of Motor-Vehicle Air Pollution. Publication No. UCD-ITS-RR-96-03(11), Institute of Transportation Studies, University of California at Davis.

Merz, P.H., Painter, L.J., Ryason, P.R., 1972. Aerometric data analysis–time series analysis and forecast and an atmospheric smog diagram. Atmospheric Environment 6, 319–342.

NAAQS, 2006. National Ambient Air Quality Standards. US EPA. 〈http://www.epa.gov/air/criteria.html〉. Accessed on 5/31/2006.

NRC, 1991. Rethinking the Ozone Problem in Urban and Regional Air Pollution. National Research Council, National Academy Press, Washington, DC.

NRC, 2004. The Hydrogen Economy: Opportunities, Costs, Barriers, and R&D Needs. National Research Council—Board on Energy and Environmental Systems, Washington, DC.

Ogden, J.M., 1999. Prospects for Building a Hydrogen Energy Infrastructure. final draft report, Center for Energy and Environmental Studies, Princeton University.

Ogden, J.M., 2002. Hydrogen: the fuel of the future? Physics Today, 69–75.

Ogden, J.M., Williams, R.H., Larson, E.D., 2004. Societal lifecycle costs of cars with alternative fuels/engines. Energy Policy 32, 7–27.

Seinfeld, J.H., Pandis, S.N., 1998. Atmospheric Chemistry and Physics: From Air Pollution to Climate Change. Wiley, NY.

Sperling, D., Ogden, J.M., 2004. The hope for hydrogen. Issues in Science and Technology, 82–86.

TMY2, 2006. National Renewable Energy Laboratory (NREL). 〈http://rredc.nrel.gov/solar/pubs/tmy2/〉. Accessed on 5/25/2006.

Wang, G., Delucchi, M.A., 2005. Lifecycle Emissions Model (LEM): Lifecycle Emissions from Transportation Fuels, Motor Vehicles, Transportation Modes, Electricity Use, Heating and Cooking Fuels, and Materials, APPENDIX X: Pathways Diagrams. Publication No. UCD-ITS-RR-03-17X, Institute of Transportation Studies, University of California at Davis.

Wang, G., Ogden, J.M., Nicholas, M.A., 2007. Lifecycle impacts of natural gas to hydrogen pathways on urban air quality. International Journal of Hydrogen Energy, in press. doi:10.1016/j.ijhydene.2007.01.006.